European Radiology (2023) 33:7923–7933
https://doi.org/10.1007/s00330-023-09755-1

European Radiology
ESR EUROPEAN SOCIETY OF RADIOLOGY

HEAD AND NECK

Intracranial aneurysms treated with stent-assisted coil embolization: evaluation with four-dimensional ultrashort-TE MR angiography

Hiroyuki Uetani[1] · Mika Kitajima[1,2] · Yuki Ohmori[3] · Kosuke Morita[4] · Yuichi Yamashita[5] · Yasuyuki Kaku[3] · Takeshi Nakaura[1] · Akira Sasao[1,6] · Goh Sasaki[1] · Soichiro Ishiuchi[1] · Akitake Mukasa[3] · Toshinori Hirai[1]

Received: 31 October 2022 / Revised: 23 February 2023 / Accepted: 10 March 2023 / Published online: 7 June 2023

Abstract

Objectives As a novel follow-up method for intracranial aneurysms treated with stent-assisted coil embolization (SACE), we developed four-dimensional magnetic resonance angiography (MRA) with minimized acoustic noise utilizing ultrashort-echo time (4D mUTE-MRA). We aimed to assess whether 4D mUTE-MRA is useful for the evaluation of intracranial aneurysms treated with SACE.

Methods This study included 31 consecutive patients with intracranial aneurysm treated with SACE who underwent 4D mUTE-MRA at 3 T and digital subtraction angiography (DSA). For 4D mUTE-MRA, five dynamic MRA images with a spatial resolution of $0.5 \times 0.5 \times 0.5$ mm^3 were obtained every 200 ms. Two readers independently reviewed the 4D mUTE-MRA images to evaluate the aneurysm occlusion status (total occlusion, residual neck, and residual aneurysm) and the flow in the stent using a 4-point scale (from 1 [not visible] to 4 [excellent]). The interobserver and intermodality agreement was assessed using κ statistics.

Results On DSA images, 10 aneurysms were classified as total occlusion, 14 as residual neck, and 7 as residual aneurysm. In terms of aneurysm occlusion status, the intermodality and interobserver agreement was excellent ($\kappa = 0.92$ and $\kappa = 0.96$, respectively). For the flow in the stents on 4D mUTE-MRA, the mean score was significantly higher for single stents than multiple stents ($p < .001$) and for open-cell type stents than closed-cell type ($p < .01$).

Conclusions 4D mUTE-MRA is a useful tool with a high spatial and temporal resolution for the evaluation of intracranial aneurysms treated with SACE.

Key Points

- *In the evaluation of intracranial aneurysms treated with SACE on 4D mUTE-MRA and DSA, the intermodality and interobserver agreement in aneurysm occlusion status was excellent.*
- *4D mUTE-MRA shows good to excellent visualization of flow in the stents, especially for cases treated with a single or open-cell stent.*
- *4D mUTE-MRA can provide hemodynamic information related to embolized aneurysms and the distal arteries to stented parent arteries.*

Keywords Magnetic resonance imaging · Magnetic resonance angiography · Stents · Intracranial aneurysm

✉ Hiroyuki Uetani
hama-moto@hotmail.co.jp

[1] Departments of Diagnostic Radiology, Faculty of Life Sciences, Kumamoto University, 1-1-1, Honjo, Chuou-ku, Kumamoto, Japan

[2] Department of Medical Image Sciences, Faculty of Life Sciences, Kumamoto University, 1-1-1, Honjo, Chuou-ku, Kumamoto, Japan

[3] Department of Neurosurgery, Faculty of Life Sciences, Kumamoto University, 1-1-1, Honjo, Chuou-ku, Kumamoto, Japan

[4] Central Radiology Section, Kumamoto University Hospital, 1-1-1, Honjo, Chuou-ku, Kumamoto, Japan

[5] Canon Medical Systems Corporation, MRI Sales Department, Sales Engineer Group, 70-1, Yanagi-cho, Saiwai-ku, Kawasaki, Kanagawa 212-0015, Japan

[6] Joint Research Course of Imaging Dynamics Applied Medicine, Faculty of Life Sciences, Kumamoto University, 1-1-1, Honjo, Chuou-ku, Kumamoto, Japan

Abbreviations

ASL	Arterial spin-labeling
DSA	Digital subtraction angiography
IC-PC	Internal carotid-posterior communicating artery
MRA	Magnetic resonance angiography
mUTE-MRA	Minimized acoustic noise utilizing UTE combined with an ASL technique
LVIS	Low-profile Visualized Intraluminal Support
PETRA	Pointwise encoding time reduction with radial acquisition
SACE	Stent-assisted coil embolization
TI	Inversion time
TOF	Time-of-flight
UTE	Ultrashort-echo time

Introduction

Stent-assisted coil embolization (SACE) has been used to treat intracranial aneurysms, particularly wide-neck aneurysms [1]. Post-treatment follow-up is important due to the risk of aneurysmal enlargement caused by coil compaction or incomplete embolization and in-stent stenosis after SACE. Approximately 8.1–12% of patients with intracranial aneurysms presented with recanalization after SACE [2, 3]. Digital subtraction angiography (DSA) is the gold standard follow-up examination after treatment with SACE. However, it has some risks associated with catheterization, radiation exposure, and the use of iodinated contrast media [4–6]. Therefore, a noninvasive imaging method is required to follow up patients treated with SACE.

Three-dimensional (3D) time-of-flight (TOF) magnetic resonance angiography (MRA) is widely used to evaluate cerebral vascular diseases. Moreover, it is considered a noninvasive alternative to DSA [7–9]. Several studies have reported that flow in the stent is challenging to visualize using TOF-MRA due to magnetic susceptibility and radiofrequency shielding, and its use in assessing residual flow in aneurysms is controversial [9, 10]. Recently, 3D ultrashort-echo time (UTE)-MRA with arterial spin-labeling (ASL) has been used as a follow-up imaging tool in patients with intracranial aneurysms treated with SACE [10–13]. Because UTE reduces magnetic susceptibility artifacts in stents and coils and minimizes the phase dispersion of the labeled blood flow signal using ASL, 3D UTE-MRA can be utilized to evaluate flow in the stent and the residual flow in aneurysms. However, it has a relatively low spatial resolution (an in-plane resolution of 1×1 mm^2 or higher) and is not able to provide hemodynamic information. Recently, ASL-based four-dimensional (4D) MRA has been reported to provide high spatial and temporal resolution [14], but there are no reports of ASL-based 4D MRA combined with UTE technology.

To overcome these issues of 3D UTE-MRA, we developed a 4D MRA sequence with minimized acoustic noise utilizing UTE combined with an ASL technique (4D mUTE-MRA). It has an in-plane resolution of less than 1×1 mm^2 and is expected to be used to evaluate flow in the stent, aneurysm occlusion status, and hemodynamics of the aneurysms and adjacent arteries in the evaluation of intracranial aneurysms treated with SACE. This study aimed to determine whether 4D mUTE-MRA is useful for the evaluation of intracranial aneurysms treated with SACE.

Materials and methods

Study population

This retrospective study was approved by the institutional review board. Informed consent was obtained using the opt-out method described on our hospital Web site. One hundred-thirty consecutive patients with intracranial aneurysms treated in our institution were searched and recruited from June 2017 to January 2021 (Suppl. material). The inclusion criteria included patients who had intracranial aneurysms treated with SACE and who underwent follow-up 4D mUTE-MRA and DSA. Ninety-four patients treated with non-SACE treatment such as clipping ($n = 22$), coil embolization alone ($n = 63$), flow diverter placement ($n = 4$), and trapping ($n = 5$) were excluded. In 36 patients treated with SACE, five patients were excluded due to no 4D mUTE-MRA study within eight days after SACE ($n = 2$), stents placed in the small artery (e.g., the posterior inferior cerebellar artery) ($n = 2$), and severe metallic artifact from an aneurysm clip ($n = 1$). Finally, 31 consecutive patients (19 women; age range: 42–77 [mean: 61.8] years) with intracranial aneurysms treated with SACE were included in this study. The mean time interval between DSA and MRI was 2.0 (range, 1–8) days. These examinations were performed within 1 week after SACE.

Three types of stents were used in this study: Neuroform Atlas stent (Stryker), LVIS Jr. stent (MicroVention), and Enterprise 2VRD stent (Codman). Of the 31 patients, 24 were treated with a single stent (14 patients with Neuroform Atlas stent, 9 patients with LVIS Jr. stent, and one patient with Enterprise 2VRD stent). Six patients were

treated with two stents (one patient with two Neuroform stents, three with two LVIS stents, and two with Neuroform and LVIS stents), and one with three LVIS stents. The aneurysms were located at the paraclinoid portion of the internal carotid artery (ICA) ($n=7$), basilar top ($n=6$), anterior communicating artery ($n=5$), cavernous portion of the ICA ($n=4$), ICA-posterior communicating artery (IC-PC) ($n=3$), vertebral artery ($n=3$), distal portion of the anterior cerebral artery ($n=2$), and middle cerebral artery ($n=1$). The mean aneurysm diameter was 9.7 ± 5.3 (range, 3–24) mm.

Description of the 4D mUTE-MRA technique

The 4D mUTE-MRA is a 4D ASL-based MRA sequence with minimized acoustic noise utilizing ultrashort-echo time. Figure 1 shows the architecture of 4D mUTE-MRA. It comprised multiple inversion time (TI) MRA data with signal targeting with alternating radio frequency with the asymmetric inversion slabs (mASTAR) technique combining ASL and a 3D mUTE radial acquisition readout. The ASTAR method with Look-Locker sampling was used for spin tagging [15, 16]. The vascular image with suppressing venous flow was obtained by subtracting the images acquired separately (Fig. 1A). This facilitates visualization of hemodynamics within a short period of time. The 3D mUTE radial readout was acquired at multiple TIs after a single tag pulse. Data were acquired radially from the center of k-space (Fig. 1B). Since the application of a readout gradient field during radiofrequency excitation causes signal loss at the center of k-space, the area was filled with the orthogonal acquisition (Fig. 1B).

MRI protocol

All MRI procedures were performed with a 3-T MRI system (Galan ZGO; Canon Medical Systems) and a 32-channel head coil. The parameters of the 4D mUTE-MRA sequence were as follows: TR/TE, 3.0/0.1 ms; flip angle, 6°; recovery time, 1226 ms; field of view (FOV), 250×250 mm; matrix, 256×256; section thickness, 1 mm; reconstructed spatial

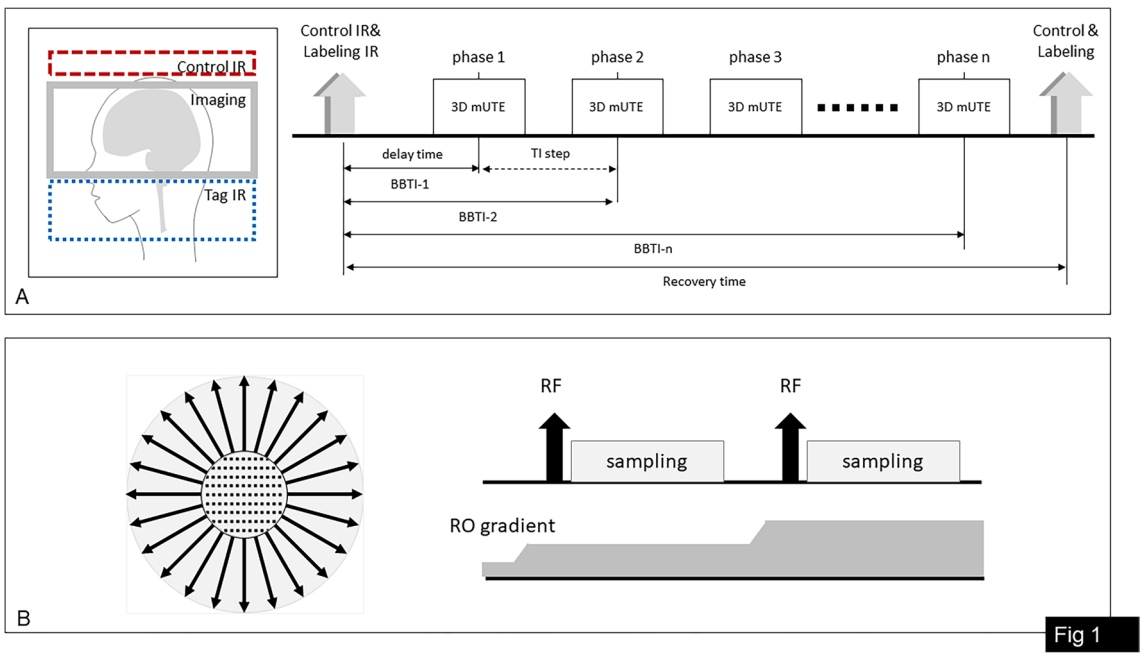

Fig. 1 Schematic labeling geometry and pulse sequence diagram of the four-dimensional (4D) mUTE-MRA technique. **A** 4D mUTE-MRA comprises multiple inversion time MRA with signal targeting with alternating radio frequency with the asymmetric inversion slabs technique combining the pulsed arterial spin-labeling technique and a three dimensional (3D) mUTE radial acquisition readout. The control and tag inversion recovery pulses were applied, as shown in the figure. The vascular image was obtained by subtracting the images acquired separately with suppressing venous flow. A 3D mUTE radial readout was acquired at multiple TIs after a single tag pulse. **B** mUTE is a silent 3D acquisition with a constant readout gradient field applied during acquisition and a slight switching of the gradient field just before radiofrequency excitation. Data were acquired radially from the center of k-space. Since the application of a readout gradient field during radiofrequency excitation causes signal loss at the center of k-space, which is the area filled with point by point on a cartesian trajectory. BBTI = blood–blood inversion time

resolution, $0.5 \times 0.5 \times 0.5$ mm^3; number of excitations, 2; parallel imaging factor, 1; delay time, 200 ms; inversion time step, 200 ms; number of acquisition phase, 5 (200, 400, 600, 800, and 1000 ms); number of segmentation, 160; number of trajectories, 9600; bandwidth, 244 kHz; and acquisition time, 9 min. The maximum intensity projection technique was used for the 3D display of MRA images. In each case, five dynamic MRA images were created to match the DSA view, which is optimal for the evaluation of embolized aneurysms. In addition, five dynamic MRA images were integrated to reconstruct the MRA images with three orthogonal planes.

DSA protocol

Biplanar intra-arterial DSA (Allura Clarity FD 20/15; Philips Medical Systems, Best, the Netherlands) was performed via a femoral artery approach by trained neurosurgeons. Iodinated contrast medium (Iopamidol, Iopamiron 300; Bayer-Schering) at 6–10 mL was selectively administered into the ICA or vertebral artery according to aneurysm location. The image matrix and FOV were 2048×2048 and 190×190 mm, respectively. The temporal resolution was three frames per second. Rotational 3D angiography was also performed for additional confirmation of the findings.

Image analysis

A neuroradiologist (T.H.) with 31 years of experience in neuroradiology assessed the visualization of aneurysm occlusion status and the lumen in the stents on DSA at a picture archiving and communication system workstation (PACS). The reader classified the aneurysm occlusion status as total occlusion, residual neck, and residual aneurysm using the Raymond-Roy occlusion classification [17]. Then, the reader also rated the visualization of the lumen in each stent as follows: occlusion (no contrast filling in the stent), stenosis (good flow with slight to moderate stenosis in the stent), and no stenosis (excellent flow without stenosis in the stent).

Two readers (M.K. and H.U., with 30 and 13 years of experience in neuroradiology, respectively) independently assessed 4D mUTE-MRA (five dynamic MRA images similar to DSA projection, integrated MRA images from dynamic MRA images in three orthogonal directions, and one zoomed selective integrated MRA image similar to DSA projection) findings on a PACS. The experienced neuroradiologist who evaluated DSA findings selected these MRA images for the blinded reading study. The zoomed selective integrated MRA was created by trimming the artery overlying the aneurysm. The two readers were blinded to the DSA data, but not to those about the location of treated aneurysms. For all images, the window width and window level could be modified for assessment. Applying the Raymond-Roy occlusion classification [15] to 4D mUTE-MRA findings, the aneurysm occlusion status on 4D mUTE-MRA images was classified as total occlusion, residual neck, and residual aneurysm. A total occlusion meant no signal in the whole aneurysm. A residual neck was defined as the presence of a slight signal in the neck of the aneurysm but without a signal of the aneurysmal sac. Any signal of the aneurysmal sac was classified as a residual aneurysm. With regard to the visualization of flow in each stent on 4D mUTE-MRA images, the two readers evaluated the zoomed selective integrated MRA image similar to DSA projection in each case using a previously reported 4-point scale system [10]: grade 1, not visible (almost no signal in the stent); grade 2, poor (structures slightly visible but with significant blurring or artifacts, not diagnostic); grade 3, acceptable (acceptable-quality diagnostic information with medium blurring or artifacts); or grade 4, excellent (good-quality diagnostic information with minimal blurring or artifacts). Divergent assessments for aneurysm occlusion status or flow in the stent were re-evaluated by two readers to reach a consensus.

After performing the blinded independent study, the hemodynamic status of the embolized aneurysm and the arteries distal to the stented parent artery on 4D mUTE-MRA images was reviewed retrospectively by the same readers in consensus, together with the DSA findings.

Statistical analysis

The interobserver agreement for 4D mUTE-MRA with respect to aneurysm occlusion status and flow in the stent was determined by calculating the weighted κ coefficient ($\kappa < 0.20$, poor agreement; $\kappa = 0.21$–0.40, fair agreement; $\kappa = 0.41$–0.60, moderate agreement; $\kappa = 0.61$–0.80, good agreement; $\kappa = 0.81$–0.90, very good agreement; and $\kappa > 0.90$, excellent agreement) with 95% confidence intervals (CIs) (5). The intermodality agreement for the assessments of aneurysm occlusion status between 4D mUTE-MRA and DSA was determined by calculating the weighted κ coefficient. In addition, the sensitivity and specificity with 95% CIs of 4D mUTE-MRA for detecting residual neck or residual aneurysm were calculated.

For the flow in each stent on 4D mUTE-MRA images, the mean score was compared between single and multiple stents and open-cell (Neuroform Atlas) and closed-cell type (LVIS Jr. and Enterprise 2VRD) stents using the Mann–Whitney U test after assessing normality using the Shapiro-Wilk test. A p value of <0.05 was considered statistically significant. MedCalc for Windows (MedCalc Software) was used for all analyses.

Table 1 Summary of visual assessments of aneurysm occlusion status

Aneurysm occlusion status	4D mUTE-MRA		Interobserver agreement[a]	DSA	4D mUTE-MRA Consensus reading	Intermodality agreement[b]
	Observer 1	Observer 2				
Total occlusion	11	11	$\kappa = 0.96$ [0.88–1.00]	10	11	$\kappa = 0.92$ [0.81–1.00]
Residual neck	11	12		14	12	
Residual aneurysm	9	8		7	8	

4D mUTE-MRA indicates four-dimensional magnetic resonance angiography with minimized acoustic noise utilizing ultrashort-echo time combined with a pulsed arterial spin-labeling technique. DSA means digital subtraction angiography. Data are number of aneurysms. κ indicates κ statistics value, with 95% confidence intervals in parentheses

[a]Agreement of 4D mUTE-MRA between observer 1 and observer 2

[b]Agreement between the consensus reading at 4D mUTE-MRA of observer 1 and observer 2 and DSA

Results

On DSA images, 10 aneurysms were classified as total occlusion, 14 as residual neck, and 7 as residual aneurysm. The interobserver agreement for the evaluation of aneurysm occlusion status on 4D mUTE-MRA images was excellent ($\kappa = 0.96$; 95% CI: 0.88, 1.00). The intermodality agreement between DSA and 4D mUTE-MRA findings was excellent for the evaluation of aneurysm occlusion status ($\kappa = 0.92$; 95% CI: 0.81, 1.00) (Table 1, Figs. 2, 3, 4, and 5). Consensus readings at 4D mUTE-MRA of observer 1 and observer 2 had a sensitivity of 100% (95% CI: 83.2%, 100%) and

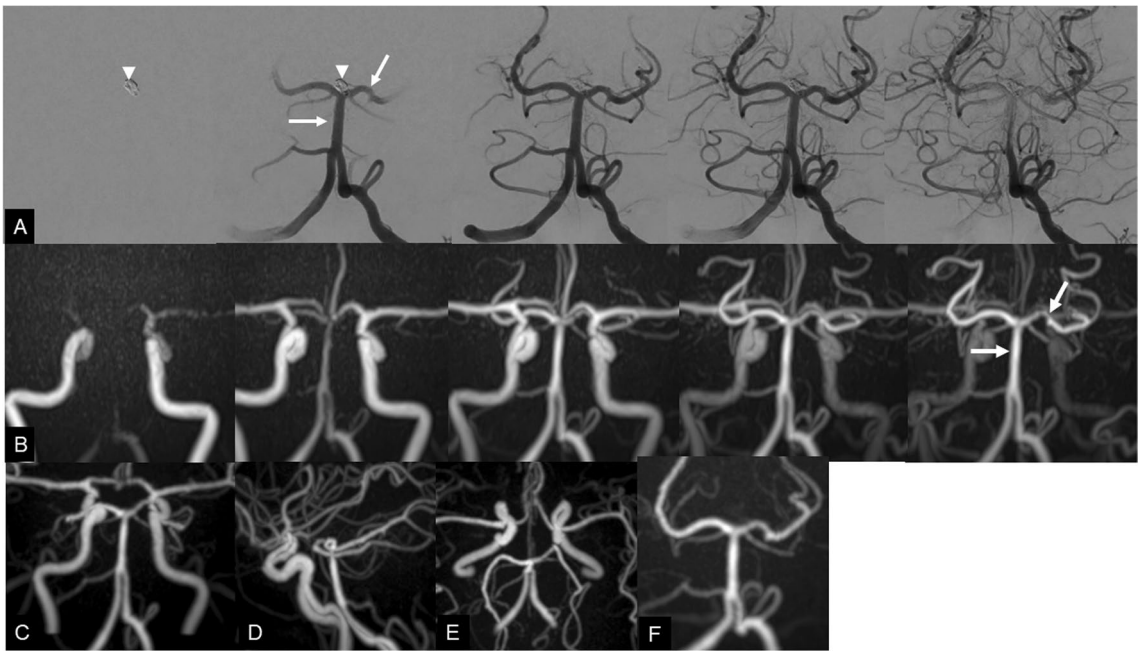

Fig. 2 A 60-year-old man treated with stent-assisted coil embolization of the basilar top aneurysm with a single Neuroform Atlas stent. **A**, Anteroposterior projections of digital subtraction angiography images of the left vertebral artery with a temporal resolution of 333 ms show total occlusion of the basilar top aneurysm (arrowheads) and excellent flow without stenosis in the stent. Arrows indicate the stent edges. **B**, Anteroposterior maximum intensity projections of four-dimensional magnetic resonance angiography (MRA) with minimized acoustic noise utilizing ultrashort-echo time (4D mUTE-MRA) (3D mUTE-MRA images with a temporal resolution of 200 ms) show no signal in the aneurysm, an excellent flow signal in the stent, and antegrade flow from the parent artery stented to the distal arteries. Arrows indicate the stent edges. Anteroposterior (**C**), lateral (**D**), and axial (**E**) maximum intensity projections of integrated 4D mUTE-MRA images made from five dynamic MRA images and zoomed selective integrated MRA image similar to DSA projection (**F**) also show no signal in the aneurysm and an excellent flow signal in the stent. In the findings of 4D mUTE-MRA images, both observers assigned total occlusion for aneurysm occlusion status and grade 4 for flow in the stent

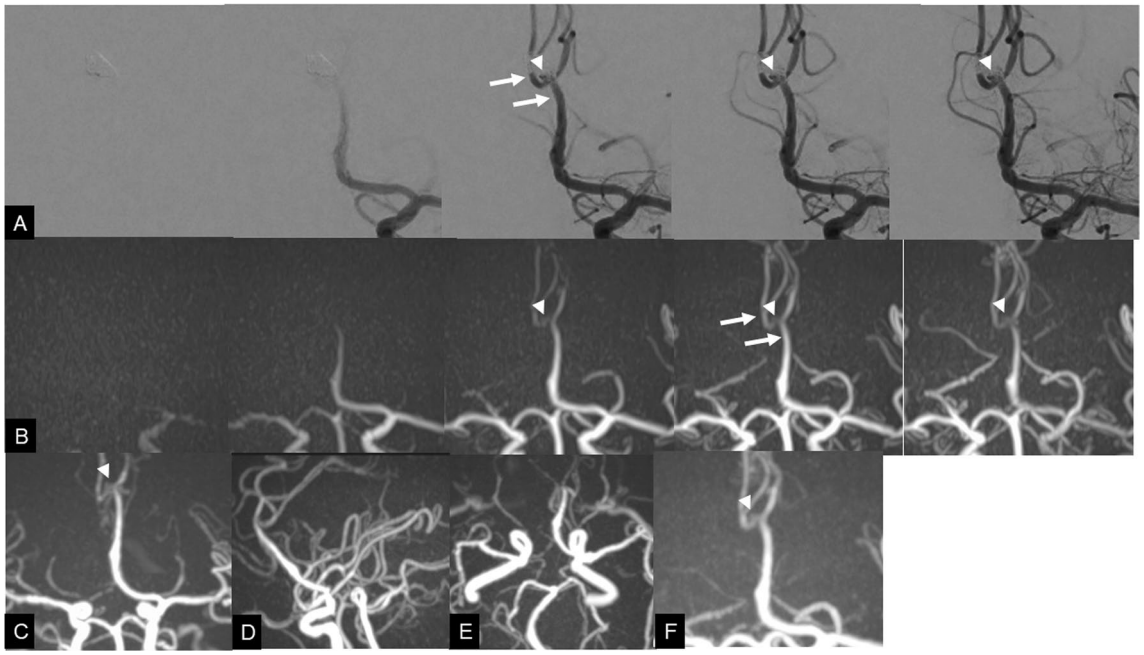

Fig. 3 A 70-year-old man treated with stent-assisted coil embolization of the distal anterior cerebral artery aneurysm with a single Neuroform Atlas stent. **A** Anteroposterior projections of digital subtraction angiography images of the left internal carotid artery with a temporal resolution of 333 ms show residual neck of the aneurysm (arrowheads) and excellent flow without stenosis in the stent. Arrows indicate the stent edges. **B** Anteroposterior maximum intensity projections of four-dimensional magnetic resonance angiography (MRA) with minimized acoustic noise utilizing ultrashort-echo time (4D mUTE-MRA) with a temporal resolution of 200 ms show equivocal residual neck of the aneurysm (arrowheads), an excellent flow signal in the stent, and antegrade flow from the parent artery stented to the distal arteries. Arrows indicate the stent edges. Anteroposterior (**C**), lateral (**D**), and axial (**E**) maximum intensity projections of integrated 4D mUTE-MRA images made from five dynamic MRA images and zoomed selective integrated MRA image similar to DSA projection (**F**) show excellent flow in the stent. Anteroposterior projection of integrated MRA (**C**) and zoomed selective integrated MRA images (**F**) show residual neck of the aneurysm (arrowheads). In the assessment of 4D mUTE-MRA findings, both observers assigned residual neck for aneurysm occlusion status and grade 4 for flow in the stent

a specificity of 91% (95% CI: 58.7%, 99.8%) for detecting residual neck or residual aneurysm.

On DSA images, the lumen in the stents of all 31 patients treated with SACE had an excellent flow without stenosis. The summary of the evaluation for the flow in the stent on 4D mUTE-MRA images is shown in Table 2. The representative cases for the flow in the stent on 4D mUTE-MRA images are indicated in Fig. 6. The interobserver agreement for the flow in the stents was very good in 4D mUTE-MRA ($\kappa = 0.83$; 95% CI: 0.69, 0.96). In 4D mUTE-MRA, two observers judged the flow in the stent to be grade 3 or grade 4 in 23 and 22 patients, respectively. Three patients evaluated as grade 1 by either of the two observers had two or three LVIS stents (Fig. 6A). The mean score for the flow in the stents was significantly higher for the single than the multiple stents (observer 1, 3.29 ± 0.69 and 2.00 ± 0.82, $p < 0.01$; observer 2, 3.21 ± 0.72 and 2.14 ± 1.07, $p = 0.015$). It was also significantly higher for the open-cell type stent than the closed-cell type (observer 1, 3.60 ± 0.51 and 2.43 ± 0.85, $p < 0.01$; observer 2, 3.53 ± 0.64 and 2.45 ± 0.85, $p < 0.01$).

In this retrospective study, residual flow in the aneurysmal sac (residual aneurysm) was observed in eight cases for 4D mUTE-MRA and in seven cases for DSA. In one case with dissociated findings between the two modalities, a left proximal middle cerebral artery aneurysm treated with SACE using a single LVIS Jr was classified as a residual aneurysm for 4D mUTE-MRA and a residual neck for DSA (Fig. 4). In six out of eight (75%) cases with a residual aneurysm on 4D mUTE-MRA, the volume of the residual lumen was judged to be larger for 4D mUTE-MRA than DSA (Fig. 5). Additionally, the size and signal of the residual lumen of the aneurysm varied sequentially from early to late in the arterial phase on 4D mUTE-MRA images, where the same information was not obtained by DSA (Fig. 5). In the remaining two cases, the volume of the residual lumen was judged to be equivalent between 4D mUTE-MRA and DSA. The antegrade flow from the parent artery stented to

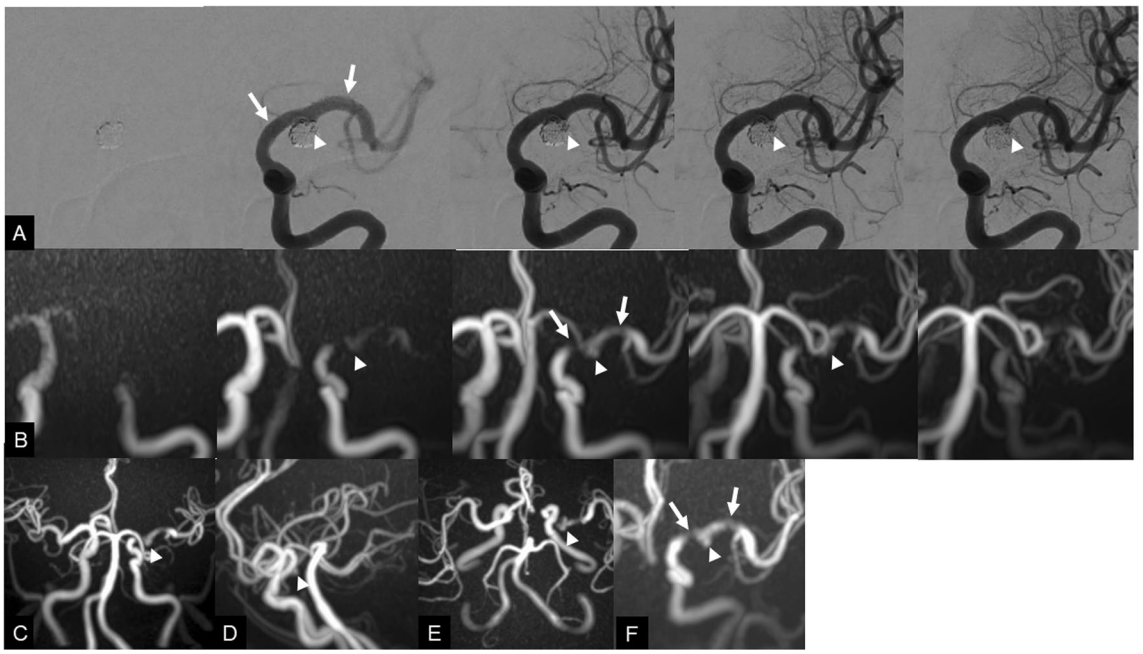

Fig. 4 A 72-year-old woman treated with stent-assisted coil embolization of the left proximal middle cerebral artery aneurysm with a single LVIS Jr. stent. **A** Anteroposterior projections of digital subtraction angiography images of the left internal carotid artery with a temporal resolution of 333 ms show small residual flow (arrowheads) near the neck and excellent flow without stenosis in the stent. Arrows indicate the stent edges. **B** Anteroposterior maximum intensity projections of four-dimensional magnetic resonance angiography (MRA) with minimized acoustic noise utilizing ultrashort-echo time (4D mUTE-MRA) images with a temporal resolution of 200 ms show a protrusion of the residual lumen into the coil mass (arrowheads) and antegrade flow from the parent artery stented to the distal arteries. Anteroposterior (**C**), lateral (**D**), and axial (**E**) maximum intensity projections of integrated MRA images made from five dynamic MRA images and zoomed selective integrated MRA image similar to DSA projection (**F**) show a protrusion of the residual aneurysm into the coil mass (arrowheads) and a signal loss in the stent edges (arrows). In the findings of 4D mUTE-MRA, both observers assigned residual aneurysm for aneurysm occlusion status and grade 2 for flow in the stent

the distal arteries was similar in the two types of images in all cases (Figs. 2, 3, 4, and 5).

Discussion

Our study findings indicated that 4D mUTE-MRA at 3 T was useful for the evaluation of intracranial aneurysms treated with SACE. Agreement between 4D mUTE-MRA and DSA findings was excellent for the evaluation of aneurysm occlusion status. We attributed these results to the high signal-to-noise ratio from the use of a 3-T MR unit and a 32-channel head coil, the high spatial and temporal resolution ($0.5 \times 0.5 \times 0.5$ mm^3 and 200 ms per volume) of the MRA technique, decreased magnetic susceptibility from UTE, and lower phase dispersion of labeled blood flow signal using the ASL technique. To our knowledge, our study is the first documentation showing the efficacy of 4D UTE-based MRA for the evaluation of intracranial aneurysms treated with SACE.

Coil artifacts in cerebral aneurysms depend on the coil material and TE, and the use of a shorter echo time on TOF-MRA and platinum:iridium coils has been reported to produce less artifact [18, 19]. Recent studies showed a good correlation between DSA and 3D UTE-MRA for the evaluation of aneurysm occlusion status of intracranial anterior circulation aneurysms treated with SACE based on a 2-point scale (total occlusion or residual neck/aneurysm) [10, 20]. Takano et al [10] reported excellent intermodality agreements between DSA and Silent MRA in 31 patients treated with LVIS stents (21 patients treated with a single stent and 10 treated with 2 stents). Heo et al [16] also reported good to excellent intermodality agreements between DSA and 3D UTE-MRA using the pointwise encoding time reduction with radial acquisition (PETRA) in 25 patients treated with Neuroform stent and Enterprise stent (24 patients treated with a single stent and 1 treated with 2 stents). Although our result seems to be similar to the previous results using 3D UTE-MRA, it is difficult to compare our results with those of these studies because there

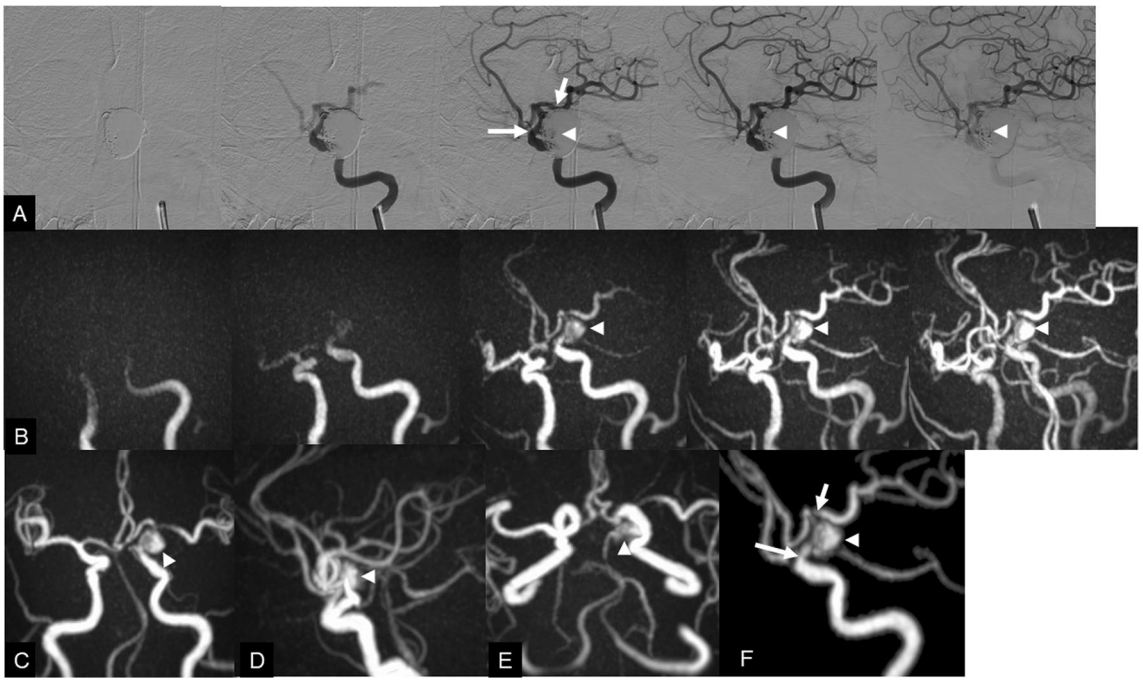

Fig. 5 A 63-year-old woman treated with stent-assisted coil embolization of the left internal carotid-posterior communicating artery aneurysm with a single LVIS Jr. stent. **A** Left anteroposterior oblique projections of digital subtraction angiography (DSA) images of the left internal carotid artery with a temporal resolution of 333 ms show residual flow in the aneurysm sac (arrowheads). Flow in the stent could not be evaluated on this view, but there was excellent flow without stenosis in the stent on another view (not shown). Arrows indicate the stent edges. **B** Left anteroposterior oblique maximum intensity projections of 4D mUTE-MRA images with a temporal resolution of 200 ms reveal a larger residual lumen in the coil mass (arrowheads) compared to DSA. The size and signal of the residual lumen of the aneurysm are changed on 4D mUTE-MRA images. The 4D mUTE-MRA images show a good flow signal in the stent, and antegrade flow from the parent artery stented to the distal arteries. Arrows indicate the stent edges. Anteroposterior (**C**), lateral (**D**), and axial (**E**) maximum intensity projections of integrated MRA images made from five dynamic MRA images and zoomed selective integrated MRA image similar to DSA projection (**F**) also demonstrate an obvious residual aneurysm (arrowheads). Zoomed selective integrated MRA image (**F**) show a slight signal loss in the stented area (arrows). In the findings of 4D mUTE-MRA, both observers assigned residual aneurysm for aneurysm occlusion status and grade 3 for flow in the stent

are several differences between our study and previous studies, e.g., aneurysm location (anterior and posterior circulation vs anterior circulation), stent types and number, acquisition type of UTE-MRA sequence (4D vs 3D), spatial and temporal resolution of MRA techniques, and a grading scale to evaluate aneurysm occlusion status (a 3-point scale vs a 2-point scale).

Our study demonstrated that the visualization of flow in the stents on 4D mUTE-MRA images depended on the cell design and the number of the stent. 4D mUTE-MRA showed good to excellent visualization of flow in the stents, especially for cases treated with a single or open-cell stent. Several previous studies have shown the efficacy of 3D UTE-MRA techniques (e.g., silent MRA, PETRA MRA) for evaluating flow in the stents after SACE [10–13, 20]. In addition, MRA signal loss due to the stent has been reported, and the cause of the signal loss is believed to be related to the material of the stent, the design of the stent cell, the thickness of the strut, and the diameter of the stent [10, 11, 21–25]. Neuroform Atlas is an opened-cell design stent with stainless steel and platinum makers [23, 26], whereas Enterprise 2VRD is a closed-cell design stent with tantalum markers [9, 27]. LVIS Jr. is also a closed-cell design self-expandable nitinol single-wire braided stent with higher metal coverage [28, 29]. Recent studies on 3D UTE-MRA reported that the closed-cell stent design and higher stent strut thickness might have more influence on stent-induced MRA signal loss [13, 21]. These results with TOF-MRA, contrast-enhanced MRA, and 3D UTE-MRA are consistent with those of our 4D mUTE-MRA study. Although these results using 3D UTE-MRA are in line with our results using 4D mUTE-MRA, their MRA sequences did not provide hemodynamic information of the embolized aneurysm and the adjacent and distal arteries.

Table 2 Summary of evaluation for the flow in the stents

Stent condition (Number of cases)	Any type of stent ($n=31$)			Open-cell stent ($n=15$)			Closed-cell stent ($n=14$)			Both types of stents ($n=2$)			single stent ($n=24$)			multiple stents ($n=7$)		
	4D mUTE-MRA		Interobserver agreement	4D mUTE-MRA		Interobserver agreement	4D mUTE-MRA		Interobserver agreement	4D mUTE-MRA		Interobserver agreement	4D mUTE-MRA		Interobserver agreement	4D mUTE-MRA		Interobserver agreement
	Ob 1	Ob 2		Ob 1	Ob 2		Ob 1	Ob 2		Ob 1	Ob 2		Ob 1	Ob 2		Ob 1	Ob 2	
Grade 4	10	10	$\kappa=0.83$ [0.69–0.96]	9	9	$\kappa=0.63$ [0.31–0.96]	1	1	$\kappa=0.84$ [0.64–1.0]	0	0	$\kappa=1.0$ [1.0–1.0]	10	9	$\kappa=0.88$ [0.71–1.0]	0	1	$\kappa=0.55$ [0.20–0.91]
Grade 3	13	12		6	5		6	6		1	1		11	11		2	1	
Grade 2	6	7		0	1		5	5		1	1		3	4		3	3	
Grade 1	2	2		0	0		2	2		0	0		0	0		2	2	
Mean score ± SD	3.00 ± 0.89	2.97 ± 0.91		3.60 ± 0.51[a]	3.53 ± 0.64[b]		2.43 ± 0.85[a]	2.43 ± 0.85[b]		2.50 ± 0.70	2.50 ± 0.70		3.29 ± 0.69[c]	3.21 ± 0.72[d]		2.00 ± 0.82[c]	2.14 ± 1.07[d]	

Data is presented as number of patients. κ indicates κ statistics value, with 95% confidence intervals in parentheses

[a,b]The mean score for the flow in the stents was significantly higher for open-cell (Neuroform Atlas) than closed-cell type (LVIS Jr. and Enterprise 2VRD) stents ($p<0.05$)

[c,d]The mean score for the flow in the stents was significantly higher for the single than the multiple stents ($p<0.05$)

Our retrospective study revealed that in six of eight (75%) cases with a residual aneurysm on 4D mUTE-MRA, the volume of the residual lumen was judged to be larger for 4D mUTE-MRA than DSA (Fig. 5). In one case, an aneurysm classified as a residual neck on DSA was scaled as a residual aneurysm on 4D mUTE-MRA (Fig. 4). Additionally, the size and signal of the residual lumen of the aneurysm varied sequentially from early to late in the arterial phase on 4D mUTE-MRA images, which information was not obtained by DSA (Fig. 5). Previous studies for evaluating intracranial aneurysms treated with coil embolization also reported larger remnants on 3-T Time-of-flight MRA, contrast enhanced-MRA, or Silent MRA than on DSA [19, 30]. Agid et al [31] reported contrast-enhanced MRA was superior to DSA for evaluation of residual aneurysm treated with coil embolization. In addition, they found a "helmet" style remnant with protrusion of the residual aneurysm into the coil mass. Shankar et al [32] also showed a case with helmet-type remnant on contrast enhanced-MRA in a patient with intracranial aneurysm after coil embolization. Takano et al [10] demonstrated three cases of a remnant with protrusion of the residual aneurysm into the coil mass on Silent MRA. This difference in the visualization of remnants is caused by a lack of X-ray penetration of the coil mass itself on DSA [10, 31]. Our results also suggest that 4D mUTE-MRA may be more useful for assessing remnants of aneurysms treated with SACE than DSA. The information on 4D mUTE-MRA images not available with DSA may be helpful for predicting aneurysm recurrence and for embolization strategies. Further studies are required to clarify the clinical value of 4D mUTE-MRA.

Additionally, 4D mUTE-MRA could provide hemodynamic information about antegrade flow from the parent artery stented to the distal arteries similar to DSA. Previous studies reported 1.2–2.5% of in-stent stenosis after SACE [2, 33]. Although there were no cases of in-stent stenosis in our study, 4D mUTE-MRA might be used to assess in-stent stenosis and delayed flow in the distal arteries.

The current study had several limitations. First, this was a single-center study with a relatively small number of patients. However, the results warrant further multicenter studies to investigate the clinical value of 4D mUTE-MRA in assessing intracranial aneurysms with SACE. Second, we did not compare 4D mUTE-MRA with 3D UTE-MRA because of the limited MRI examination time of the patients. Further studies comparing 4D mUTE-MRA with 3D UTE-MRA may be needed to clarify the clinical value of 4D mUTE-MRA.

In conclusion, the findings of the interobserver agreement on 4D mUTE-MRA and the intermodality

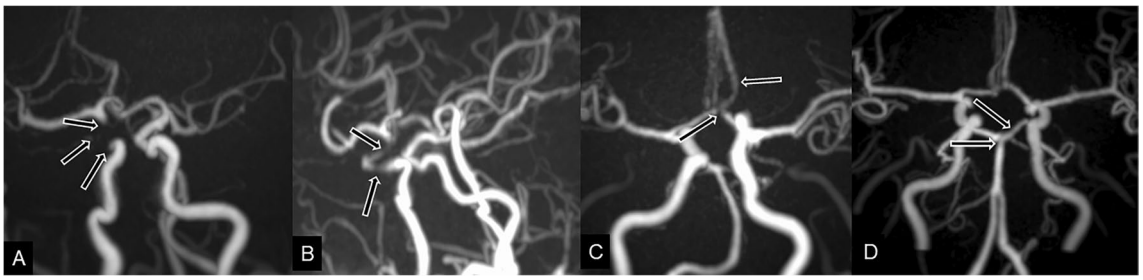

Fig. 6 The representative cases for the flow in the stent on maximum intensity projections of integrated four-dimensional magnetic resonance angiography with minimized acoustic noise utilizing ultrashort-echo time (4D mUTE-MRA). **A** A 43-year-old man treated with stent-assisted coil embolization (SACE) of the right paraclinoid internal carotid artery aneurysm with triple LVIS stents. Both observers assigned grade 1 for flow in the stents. **B** A 76-year-old woman treated with SACE of the right paraclinoid internal carotid artery aneurysm with a single LVIS stent. Both observers assigned grade 2 for flow in the stent. **C** A 44-year-old man treated with SACE of the anterior communicating artery aneurysm with double Neuroform Atlas stents. Each observer rated flow in the stents as grade 3 and grade 4, respectively. **D** A 60-year-old man treated with SACE of the basilar top aneurysm with a single Neuroform Atlas stent. Both observers assigned grade 4 for flow in the stent

agreement between 4D mUTE-MRA and DSA were excellent for aneurysmal occlusion status after SACE. 4D mUTE-MRA showed good to excellent visualization of flow in the stents, especially for cases treated with a single or open-cell stent. Thus, 4D mUTE-MRA helps evaluate intracranial aneurysms treated with SACE without the use of contrast agents, although the scanning time is 9 min. Because 4D mUTE-MRA provides higher spatial and temporal resolution and hemodynamic information which are not obtained with 3D UTE-MRA, we recommend this technique for non-invasive follow-up monitoring of intracranial aneurysms treated with SACE.

Supplementary Information The online version contains supplementary material available at https://doi.org/10.1007/s00330-023-09755-1.

Acknowledgements The authors would like to thank Kentaro Haraoka and Takumi Saito for their technical support.

Funding The authors state that this work has not received any funding.

Declarations

Guarantor The scientific guarantor of this publication is Toshinori Hirai.

Conflict of interest Yuichi Yamashita is an employee of Canon Medical Systems. Toshinori Hirai has received research support from Canon Medical Systems. Akira Sasao is a specially appointed lecturer in the Joint Research Course of Imaging Dynamics Applied Medicine, which is financially supported by CANON MEDICAL SYSTEMS. The Canon Medical Systems had no control over the interpretation, writing, or publication of this work. The other authors declare that they have no conflicts of interest.

Statistics and biometry No complex statistical methods were necessary for this paper.

Informed consent Written informed consent was waived by the Institutional Review Board.

Ethical approval Institutional Review Board approval was obtained.

Study subjects or cohorts overlap Any study subjects or cohorts have not been previously reported.

Methodology
- retrospective
- observational
- performed at one institution

References

1. Mine B, Aljishi A, D'Harcour JB, Brisbois D, Collignon L, Lubicz B (2014) Stent-assisted coiling of unruptured intracranial aneurysms: long-term follow-up in 164 patients with 183 aneurysms. J Neuroradiol 41:322–328
2. Chalouhi N, Jabbour P, Singhal S et al (2013) Stent-assisted coiling of intracranial aneurysms: predictors of complications, recanalization, and outcome in 508 cases. Stroke 44:1348–1353
3. Lawson MF, Newman WC, Chi YY, Mocco JD, Hoh BL (2011) Stent-associated flow remodeling causes further occlusion of incompletely coiled aneurysms. Neurosurgery 69:598–603; discussion 603–594
4. Ferns SP, Sprengers ME, van Rooij WJ et al (2009) Coiling of intracranial aneurysms: a systematic review on initial occlusion and reopening and retreatment rates. Stroke 40:e523-529
5. Kanaan H, Jankowitz B, Aleu A et al (2010) In-stent thrombosis and stenosis after neck-remodeling device-assisted coil embolization of intracranial aneurysms. Neurosurgery 67:1523–1532; discussion 1532–1523
6. Mocco J, Fargen KM, Albuquerque FC et al (2011) Delayed thrombosis or stenosis following enterprise-assisted stent-coiling: is it safe? Midterm results of the interstate collaboration of enterprise stent coiling. Neurosurgery 69:908–913; discussion 913–904
7. Schaafsma JD, Velthuis BK, Majoie CB et al (2010) Intracranial aneurysms treated with coil placement: test characteristics of follow-up MR angiography–multicenter study. Radiology 256:209–218

8. Lavoie P, Gariepy JL, Milot G et al (2012) Residual flow after cerebral aneurysm coil occlusion: diagnostic accuracy of MR angiography. Stroke 43:740–746
9. Cho WS, Kim SS, Lee SJ, Kim SH (2014) The effectiveness of 3T time-of-flight magnetic resonance angiography for follow-up evaluations after the stent-assisted coil embolization of cerebral aneurysms. Acta Radiol 55:604–613
10. Takano N, Suzuki M, Irie R et al (2017) Non-contrast-enhanced silent scan mr angiography of intracranial anterior circulation aneurysms treated with a low-profile visualized intraluminal support device. AJNR Am J Neuroradiol 38:1610–1616
11. Takano N, Suzuki M, Irie R et al (2017) Usefulness of non-contrast-enhanced MR angiography using a silent scan for follow-up after Y-configuration stent-assisted coil embolization for basilar tip aneurysms. AJNR Am J Neuroradiol 38:577–581
12. Irie R, Suzuki M, Yamamoto M et al (2015) Assessing blood flow in an intracranial stent: a feasibility study of MR angiography using a silent scan after stent-assisted coil embolization for anterior circulation aneurysms. AJNR Am J Neuroradiol 36:967–970
13. Kim YN, Choi JW, Lim YC, Song J, Park JH, Jung WS (2022) Usefulness of silent MRA for evaluation of aneurysm after stent-assisted coil embolization. Korean J Radiol 23:246–255
14. Suzuki Y, Fujima N, van Osch MJP (2020) Intracranial 3D and 4D MR angiography using arterial spin labeling: technical considerations. Magn Reson Med Sci 19:294–309
15. Takakura K, Kido A, Fujimoto K et al (2016) Evaluation of appropriate readout sequence for renal MRI perfusion using ASTAR (ASL) technique. Nihon Hoshasen Gijutsu Gakkai Zasshi 72:1105–1112
16. Günther M, Bock M, Schad LR (2001) Arterial spin labeling in combination with a look-locker sampling strategy: inflow turbo-sampling EPI-FAIR (ITS-FAIR). Magn Reson Med 46:974–984
17. Roy D, Milot G, Raymond J (2001) Endovascular treatment of unruptured aneurysms. Stroke 32:1998–2004
18. Bhattacharya JJ, Siddiqui MA, Zampakis P, Jenkins S (2008) MRA artefacts with Nexus coils. Neuroradiology 50:821
19. Schaafsma JD, Velthuis BK, Vincken KL, de Kort GA, Rinkel GJ, Bartels LW (2014) Artefacts induced by coiled intracranial aneurysms on 3.0-Tesla versus 1.5-Tesla MR angiography–an in vivo and in vitro study. Eur J Radiol 83:811–816
20. Heo YJ, Jeong HW, Baek JW et al (2019) Pointwise encoding time reduction with radial acquisition with subtraction-based MRA during the follow-up of stent-assisted coil embolization of anterior circulation aneurysms. AJNR Am J Neuroradiol 40:815–819
21. You SH, Kim B, Yang KS, Kim BK, Ryu J (2021) Ultrashort echo time magnetic resonance angiography in follow-up of intracranial aneurysms treated with endovascular coiling: comparison of time-of-flight, pointwise encoding time reduction with radial acquisition, and contrast-enhanced magnetic resonance angiography. Neurosurgery 88:E179–E189
22. Choi JW, Roh HG, Moon WJ et al (2011) Time-resolved 3D contrast-enhanced MRA on 3.0T: a non-invasive follow-up technique after stent-assisted coil embolization of the intracranial aneurysm. Korean J Radiol 12:662–670
23. Choi JW, Roh HG, Moon WJ, Chun YI, Kang CH (2011) Optimization of MR parameters of 3D TOF-MRA for various intracranial stents at 3.0T MRI. Neurointervention 6:71–77
24. Wang Y, Truong TN, Yen C et al (2003) Quantitative evaluation of susceptibility and shielding effects of nitinol, platinum, cobalt-alloy, and stainless steel stents. Magn Reson Med 49:972–976
25. Cho YD, Kim KM, Lee WJ et al (2014) Time-of-flight magnetic resonance angiography for follow-up of coil embolization with enterprise stent for intracranial aneurysm: usefulness of source images. Korean J Radiol 15:161–168
26. Agid R, Schaaf M, Farb R (2012) CE-MRA for follow-up of aneurysms post stent-assisted coiling. Interv Neuroradiol 18:275–283
27. Takayama K, Taoka T, Nakagawa H et al (2011) Usefulness of contrast-enhanced magnetic resonance angiography for follow-up of coil embolization with the enterprise stent for cerebral aneurysms. J Comput Assist Tomogr 35:568–572
28. Behme D, Weber A, Kowoll A, Berlis A, Burke TH, Weber W (2015) Low-profile visualized intraluminal support device (LVIS Jr) as a novel tool in the treatment of wide-necked intracranial aneurysms: initial experience in 32 cases. J Neurointerv Surg 7:281–285
29. Möhlenbruch M, Herweh C, Behrens L et al (2014) The LVIS Jr. microstent to assist coil embolization of wide-neck intracranial aneurysms: clinical study to assess safety and efficacy. Neuroradiology 56:389–395
30. Ferre JC, Carsin-Nicol B, Morandi X et al (2009) Time-of-flight MR angiography at 3T versus digital subtraction angiography in the imaging follow-up of 51 intracranial aneurysms treated with coils. Eur J Radiol 72:365–369
31. Agid R, Willinsky RA, Lee SK, Terbrugge KG, Farb RI (2008) Characterization of aneurysm remnants after endovascular treatment: contrast-enhanced MR angiography versus catheter digital subtraction angiography. AJNR Am J Neuroradiol 29:1570–1574
32. Shankar JJ, Lum C, Parikh N, dos Santos M (2010) Long-term prospective follow-up of intracranial aneurysms treated with endovascular coiling using contrast-enhanced MR angiography. AJNR Am J Neuroradiol 31:1211–1215
33. Chalouhi N, Drueding R, Starke RM et al (2013) In-stent stenosis after stent-assisted coiling: incidence, predictors and clinical outcomes of 435 cases. Neurosurgery 72:390–396